

# FAST CHANGES OF ENERGETIC PARTICLE INTENSITY NEAR THE BOUNDARY BETWEEN THE MAGNETOTAIL AND TRAPPED REGION DURING SUBSTORM ACTIVATIONS.

L. Lazutin<sup>1</sup> and T. Kozelova

*Polar Geophysical Institute, Academia, Apatity, Murmansk Region, 184200, Russia*

*1) Now at Space Physics Department, Scobeltsyn institute for Nuclear Physics, Moscow State University, Vorobjevy Gory, 199899 Russia*

tel: +7 095 9394290/ fax: +7 095 9395034

e-mail: lazutin@srdlan.npi.msu.su/kozelova@pgi.kolasc.net.ru

A. Korth

*Max-Planck-Institute for Aeronomie, D-37191, Katlenburg-Lindau, Germany*

tel: +49 5556 979430/Fax: +49 5556 979240

e-mail: korth@sprotte.mpae.gwdg.de/korth@linmpi.mpg.de

## ABSTRACT

Energetic particle and magnetic field measurements during the CRRES 615 orbit (April 4, 1991) are selected for the study of the fine structure of a trapping boundary during multiple dropout event, when the satellite departs from the trapped particle region entering the magnetotail and returns back during substorm intensifications. It is shown that the trapping boundary is a complicated dynamic structure. Several different types of boundary crossing are described, including the events with the very fast intensity changes ( $\Delta T = 1-3s$ ).

## INTRODUCTION

Energetic particle dropout effect (DE) was first registered on the geostationary orbit [Walker *et al*, 1976, Sauvaud and Winckler, 1980, Dandouras *et al*, 1986, Baker and McPherron, 1990]. Decrease of the particle flux at the beginning of DE is associated with equatorward contraction of the plasmasheet and the

earthward motion of the trapping boundary during the substorm growth phase. Decrease of the particle flux, both electrons and ions in wide energy range is accompanied by the increase of the taillike magnetic field configuration. The recovery from dropout has been identified with the moments of the substorm onset or intensifications [Sauvaud and Winckler, 1980, Lazutin *et al*, 1984]. Two types of the recovery have been recognized, in the first type particle flux returns to the previous value, whereas in the second type shortly after recovery step, an additional increase of the flux particle is taking place similar to the substorm injection events. It is not a boundary phenomena because satellite penetrates inside the trapping region when this second step were registered. Described below events belong to the first type of DE. Also it was an event with multiple DE effects when satellite several times escape and reenter the trapping region.

Most of the studies cited above use low temporal resolution data, which do not allow to investigate fine structure of this dynamic boundary. Meanwhile this region is especially interesting because it is located close to (or can be directly associated with) such important for the understanding of the substorm physics structures, as the plasma sheet boundary layer (PSBL) and auroral oval boundary (polar arc). As the substorm onset has temporal structures of the order of first tens of second, it will be interesting to inspect DE with such fast resolution. In present work we will describe the fine

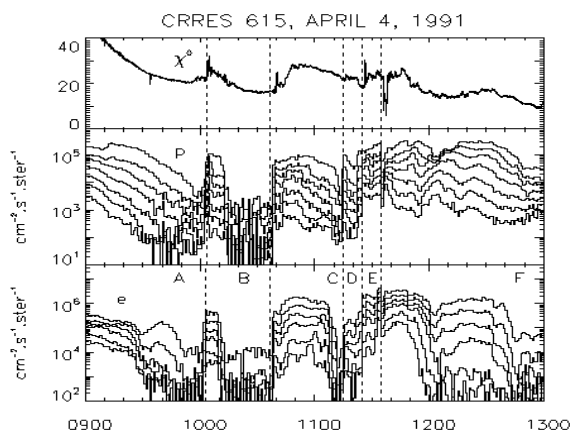


Figure 1: Multiple dropout event, April 4, 1991, the CRRES orbit 615. Upper panel: magnetic field line inclination, degrees; middle panel: Ion intensity, selected differential channels, energies from 37keV to 3.2 meV. Bottom panel: electron intensity data, 21 – 285 keV. Dropout events labeled from A to E are discussed in the text.

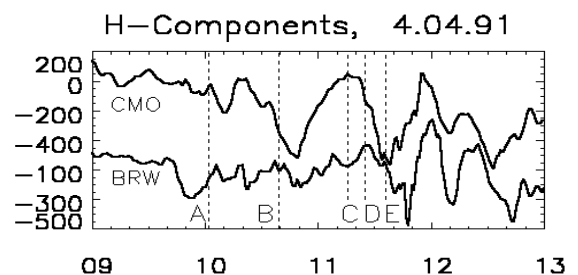


Figure 2. Magnetic field H component variations registered by College (CMO) and Barrow (BRW) magnetometers.

temporal and spatial structure of trapping boundary crossings during multiple dropout event using measurements of the energetic electrons and proton intensity by the CRRES satellite.

### OBSERVATIONS

Several dropout events were registered at April 4, 1991, when CRRES was in midnight sector at high magnetic latitude (-13°: -22°). Figure 1 presents differential flux variations in several electron and ion channels and magnetic field line inclination. DE are marked from A to F, vertical dotted lines indicate the moments of the exit from the dropout. These moments coincide with the beginning of the negative magnetic bays at the midnight sector magnetometers, as shown by Figure 2, and with partial dipolarization of the magnetic field in the vicinity of the CRRES orbit (Figure 1).

The entry into dropout may be gradual (A, D), fast (B, E) or gradual with sharp ending (C). The recoveries are usually sharp with the duration from 1-2 minutes down to 1-2 seconds. Electrons and ions are increasing simultaneously if data are averaged by 1-5 minutes, but better resolution shows different behavior with several types of the dropout recovery profiles shortly described below and illustrated by Figures 3 to 7.

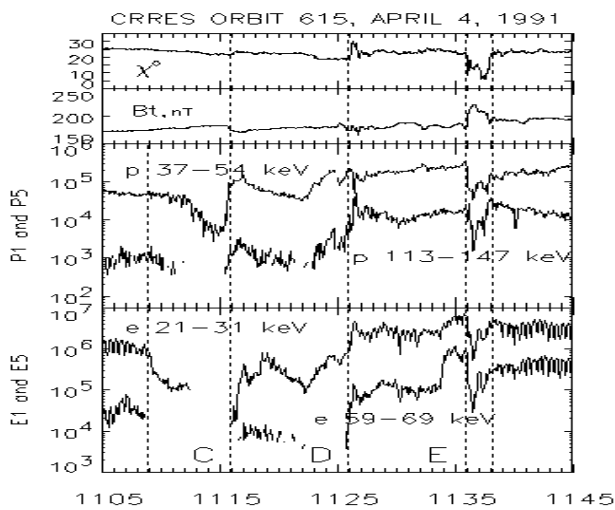


Figure 3. From top to the bottom: magnetic field line inclination, total B magnitude, Two channels both of the ion and the electron detectors during C, D and E dropout events.

*First example - different behaviour: the electrons are decreasing earlier and recovering later than the protons.* Figure 3 shows dropout C with sharp ending of the electron flux decrease at 1109 UT and delayed on several minutes ion decrease. Figure 4 shows the fine structure of the dropout C recovery at 1116 UT. It was short (2-5s) for protons and coincides with the beginning of Bt decrease, whereas the electron intensity

increase was more extended (dT=1min) and better correlated with the magnetic field dipolarization. We are using fast resolution particle data here without correction to the satellite rotation, because the PAD is nearly isotropic both in the electrons and the ions.

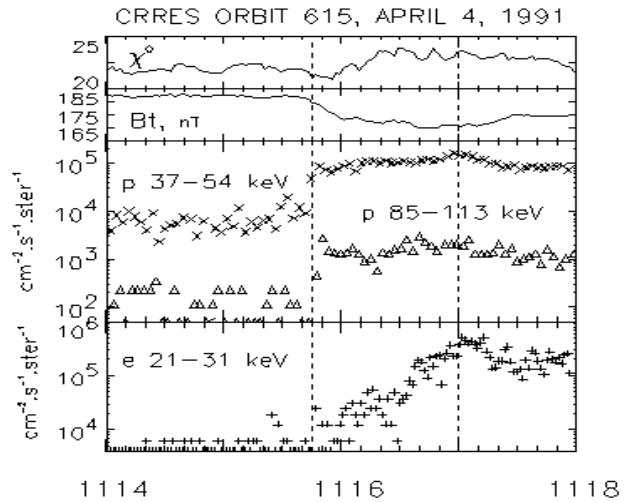


Figure 4. Fine structure of the dropout C recovery.

*Second example - correlated in general electron and ion flux variations with a difference in the activation structures.* Figure 5 present a detailed temporal structure of the recovery from the first dropout A. It was gradual, about two minutes in total, but modulated by several short bursts. There is reasonably good correlation between the electron and proton variations in a smoothed intensity increase, including higher energy channels (not shown), but detailed correlation is absent

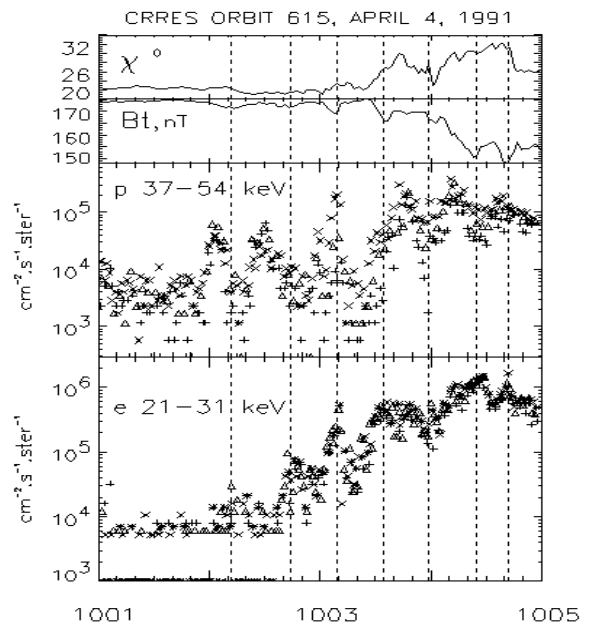


Figure 5. Fine structure of the dropout A recovery.

in a short substructure. First two pulses are in anti-correlation, bursts number 3 coincide, number 4 is delayed in the ions profile and so on. Temporal structure of the particle flux variation with irregular 15-45s periodicity is very similar to the magnetic Pi2 pulsations and associated chains of substorm activations (Lazutin, 1999). The electron intensity maxima coincide with a separate steps of the magnetic field dipolarization (decreases of the Bt indicated by the vertical dotted lines on Figure 5), whereas some proton activations profiles are shifted in time.

*Third example - detailed particle and magnetic field correlation.* From 1136 to 1138 UT the short partial dropout has been registered, associated with a sudden changes in the magnetic field topology, possibly related to the near-by field-aligned current wedge or to the propagation of some fold-like structure along the trapping boundary. It creates a synchronized drop of particle intensity, which is seen on Figure 3 and in more details on Figure 6. This decrease or drop is an excellent example of the all particles species, all energies and pitch angles correlation with  $\chi$  and B. Several smaller details of particle and field variations inside the drop are in good agreement as well. It is possible to suppose that the trapping boundary remains rather sharp this time.

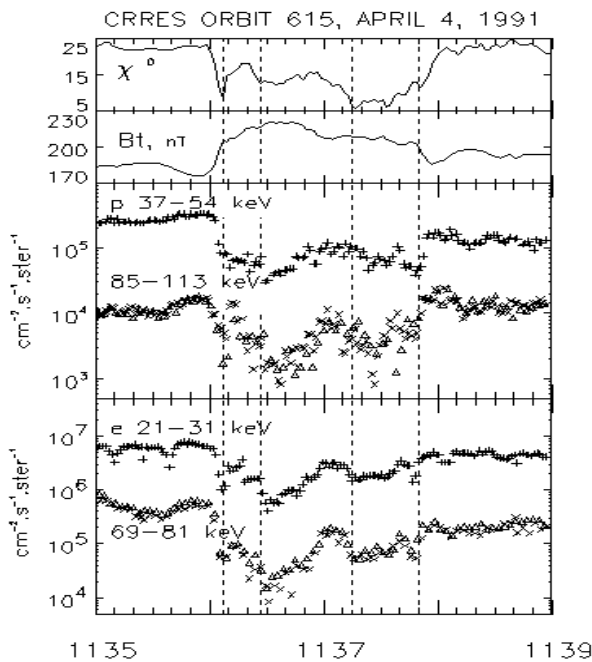


Figure 6: The short partial dropout, event D.

*Fourth example - fast correlated e and p variations.* The second recovery from the dropout (B on Fig 1 and 2) was very fast, change of the magnetic field configuration occurs in 5-6 s and was correlated with the particle intensity increase. Figure 7 shows that data of two ion and two electron energy channels and several

chosen detectors with best possible resolution. For every point of the measurements the current pitch angles of the detectors are shown with the same symbol. In the high energy electron channels an intensity increase take place in one step from the zero level (below the sensitivity threshold) for all detectors (Figure 7g). Lower energy channels, where intensity inside the dropout was above the threshold limit, show the dropout recovery with a pitch angle anisotropy. Detectors with field of view along the magnetic field line registered the first step of electrons increase before the increase of the trapped electrons and before the beginning of the magnetic field dipolarization (Figure 7f). The ions of

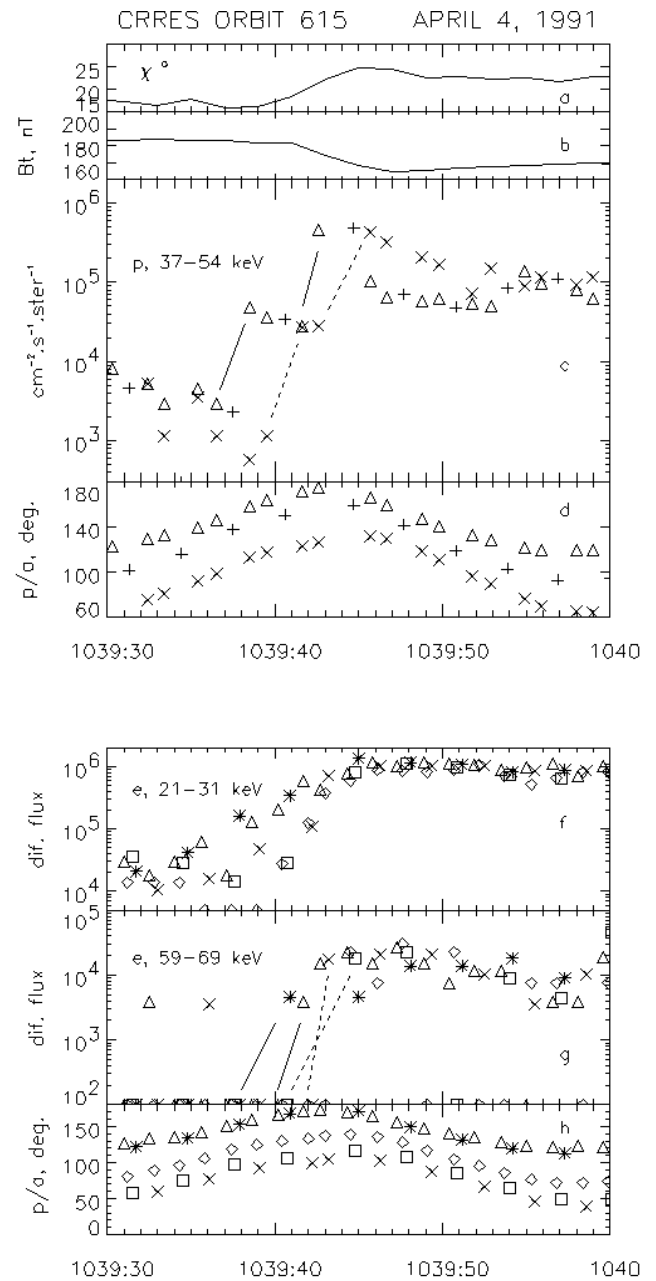


Figure 7: Fast recovery from the dropout (event B). Special panels with detectors pitch angle field of view are added. Solid and dotted lines indicate the trapped and field aligned particle increases.

all energies with a low pitch angles were arriving before the trapped particles. As shown by Figure 7c, ion intensity increase in lowest channel P1 was recorded in two steps: the first at 1039:38 UT and the second at 1039:42 UT by detector D1 (triangles, PA range: 150°-170°). Same two steps were recorded by detector D3 (x-crosses, PA range: 100°-120°) with a 3-4s delay. In higher energy channels the first jump started 1-2 s later, but the delay in arrival of the trapped protons as compared with field-aligned ones is well pronounced (not shown). There are several other examples of the pitch angle dependent increases and decreases of the particle intensity during dropout boundary passage.

Observed effects may be the consequence of the fast rotary motion of the field line tube. It became open to the tail and previously trapped particles escaped into the tail with the pitch angle dependent velocity. At the opposite rotation step previously empty field tube enters at the equator into the trapping region and we observe how the tube is filling up by energetic particles.

#### SUMMARY

The dropout effect tells us that the usual for the quite time smooth transition between dipollike and taillike magnetic field lines during disturbances became transformed into the sharp dynamic boundary. Satellite may found itself placed outside the trapping region and back several time during the composite disturbance due to the substorm related dipolarizations and tailward activity expansions and new tailward extension of the nightside magnetic field.

We presented here several examples of the temporal-spatial structure of this boundary during the dropout recoveries. If analyzed with a good time resolution, the magnetic field and the particle intensity contain reach variety of different structures. We can identify three categories: with duration of about several seconds, 15-45 s and about 100 s. These structures may be observed both in the electron and proton intensity profiles in wide energy range, but also may be different for electrons and ions, an energy dependent, and sometimes different for the different pitch angles.

Some of the effects described above may be interpreted as the reflection of the global or distant substorm activity, other are the local boundary phenomena. It is natural to assume that such boundary cannot remain smooth and stable, the instability of the ballooning type

or/and certain waves and pulses and twist motions propagating along the boundary may create observed wave-like modulated structures. The localized field-aligned current wedge described for dropout effects at the morning and evening sector (Moukis et al, 1998) may be applied at the midnight sector as well.

More extended study with additional examples of the nightside trapping boundary structure will be presented elsewhere.

#### REFERENCES

- Baker, D. N. and McPherron, R. L., Extreme energetic particle decreases near geostationary orbit: A manifestation of current diversion within the inner plasma sheet. *J. Geophysical Research*, Vol. 95, pp.6591-6599, 1990.
- Dandouras, J., Reme, H., Saint-Marc, A., et al. A statistical study of plasma sheet dynamics using ISEE 1 and 2 energetic particle flux data. *J. Geophysical Research*, Vol. 95, p 6861, 1986.
- Lazutin, L. L., Gustafsson, G., Khrushchinsky, A. A., et al., SAMBO-GEOS: Substorm trapped particle boundary movements, particle precipitation and acceleration. In: *IMS-Symposium*, Austria.: COSPAR, Graz., 1984.
- Lazutin, L. L. Substorm activations: comparison of fine structures. *Adv. Space Res.* Vol. 23, No. 10, pp. 1671-1674, 1999
- Moukis, C. G., A. Korth, R. H. W. Friedel, and J. F. Fennel, Dawn/dusk dropouts due to storms/substorms near the outer radiation belt: observations from CRRES. *Substorm-4*, edited by S. Kokubun and Y. Kamide, Terra and Kluwer Publ., Tokio, pp. 707-710, 1998.
- Sauvaud, J. A. and Winckler, J. R., Dynamics of plasma, energetic particles and fields near synchronous orbit in the nighttime sector during magnetospheric substorms, *J. Geophysical Research*. Vol. 85, pp.2043-2056, 1980.
- Walker, J. C. G., Erickson, G. M., Swanson, R. L. and Winckler, J. R., Substorm-associated particle boundary motion at synchronous orbit. *J. Geophysical Research*, Vol. 81, pp.5541-5550, 1976.